

Lifetime Measurements of Recent Microchannel-Plate PMTs

Alexander Britting*, Wolfgang Eyrich, Albert Lehmann and Fred Uhlig

Friedrich-Alexander-Univ. Erlangen (DE)

E-mail: alexander.britting@physik.uni-erlangen.de

The \bar{P} ANDA experiment at the new FAIR facility at GSI in Darmstadt requires photo sensors which will be used in the DIRC detectors for particle identification. These devices must stand integrated anode charges of 5 C/cm^2 and be able to operate in high magnetic fields. Our planned sensors are microchannel-plate (MCP) photomultipliers (PMTs), whose lifetime has increased over the last few years. We have simultaneously illuminated recent-generation devices of different manufacturers (BINP, Hamamatsu R10754X-01-M16 and PHOTONIS XP85112/H1-AGL) under conditions at high energy physics like single photon detection with a gain of at least 10^6 . Important aging parameters such as gain, dark count rate, and quantum efficiency (QE), are measured as a function of the integrated anode charge. Further the spatial QE degradation is determined in irregular intervals of several weeks. Although the illumination is still ongoing, the superior method to improve the lifetime appears to be atomic layer deposition (ALD), which is used for the XP85112/A1-HGL. In our measurements this device has passed 2.8 C/cm^2 without any sign of aging, surpassing previous MCP-PMT models by more than one order of magnitude.

International Workshop on New Photon-detectors

June 13-15, 2012

LAL Orsay, France

*Speaker.

1. Introduction

The $\bar{P}ANDA$ [1] [2] [3] experiment at GSI Darmstadt requires two state-of-the-art DIRC¹ detectors covering the central (barrel DIRC [4] [5]) and forward (disc DIRC [6]) region of the $\bar{P}ANDA$ spectrometer for pion and kaon separation of up to $4\text{ GeV}/c$. A very good separation of these particles is needed for the physics goals, such as charmonium spectroscopy and the search for exotic states. The photo sensors have to be placed inside high magnetic fields of up to 2 T, which excludes standard PMTs. Furthermore the use of SiPMs is problematic because of high neutron doses and their high dark count rates. On the other hand, MCP-PMTs are usable in the $\bar{P}ANDA$ environment [7] [8]. The high luminosity of $2 \cdot 10^{32}\text{ cm}^{-2}\text{s}^{-1}$ of $p\bar{p}$ annihilations at beam momenta of up to $15\text{ GeV}/c$ will result in photon rates of $\approx 200\text{ kHz}/\text{cm}^2$ for the barrel DIRC and even more for the disc DIRC. To achieve a good efficiency a high gain is needed. That leads to lifetime requirements of the photo sensors of $1\text{ C}/\text{cm}^2$ per year assuming 100% duty cycle and a gain of $1 \cdot 10^6$ for the barrel DIRC. Under the realistic assumption of 50% duty during the whole expected lifetime of 10 years this will result in $5\text{ C}/\text{cm}^2$ integrated anode charge for the MCPs, which was not achievable by previous models [9].

2. Setup

Four different MCP-PMTs from three different manufacturers were chosen for the aging tests: PHOTONIS XP85112/A1-HGL, Hamamatsu R10754X-01-M16, BINP #1359 and #3548. The main characteristics and some illumination parameters are listed in Table 1.

The lifetime measurement process itself was divided in several parts:

1. All devices were illuminated for several days within the same light spot to assure comparable conditions at high pulse rates of 0.27 to 1 MHz at 460 nm.

| manufacturer | Hamamatsu | PHOTONIS | BINP |
|-------------------------------|--|--|---|
| type | R10754X-01-M16 | XP85112/A1-HGL | #1359 & #3548 |
| pore size (μm) | 10 | 10 | 7 |
| pixels | 4x4 | 8x8 | 1 |
| active area (mm^2) | 22x22 | 53x53 | $9^2\pi$ |
| geom. efficiency | 61% | 81% | 36% |
| photo cathode | multi-alkali | bi-alkali | $\text{Na}_2\text{KSb}(\text{CS}) + \text{Cs}_3\text{Sb}$ |
| max. cur. per anode [nA] | 45.3 | 56 | 315/346 |
| specified max. DC cur. [nA] | 100 | 96 | 1000 |
| measured channels | 8 | 8+2 (unexposed) + MCP-Out | 1 |
| comments | protection layer between 1 st and 2 nd MCP | better vacuum; electron scrubbing; ALD | 3548 longer baked; new photo cathode |

Table 1: Overview of MCP-PMTs and illumination parameters

¹Detection of Internally Reflected Cherenkov light

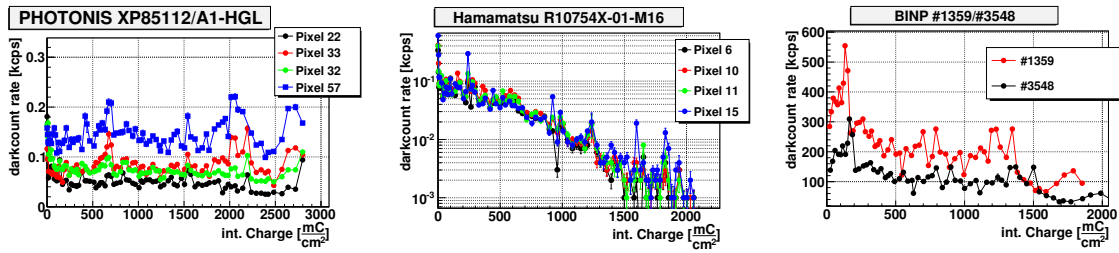


Figure 1: Dark count rates for all investigated detectors as a function of the integrated anode charge. Pixel 57 of the XP85112/A1-HGL was covered and not illuminated.

2. During an interruption the gain and dark count rate were measured. A reduced pulse rate of $5 - 10 \text{ kHz}$ for the gain measurement was used to avoid saturation effects.
3. The QE was measured in diode mode without amplification using a different setup, which will be explained later.
4. After the reassembly the gain was measured again and the aging was continued.

The light of the LED was attenuated to single photon level using neutral density filters. The repetition rate was started at 270 kHz and was increased in several steps during the measurement process to finally 1 MHz , resulting in a detected photon rate of $\sim 1 \text{ MHz/cm}^2$ for undamaged sensors. During the illumination the whole system is monitored with a photo diode and data are constantly taken at low trigger rates. Hence the collected anode charge could be calculated; at maximum it was in the order of $10 - 14 \text{ mC/cm}^2/\text{day}$ for all MCP-PMTs. The surface of all devices was fully illuminated, except that of the XP85112/A1-HGL which was half covered.

The quantum efficiency (QE) was determined by measuring the photo current in diode mode, i.e. applying ground potential to the MCPs and measuring the current. A xenon arc lamp as broadband light source in combination with a monochromator allowed measuring a spectral resolved QE of about 1 nm in the wavelength range of $200\text{-}700 \text{ nm}$. The light yield itself was determined with a calibrated photo diode². The spot diameter was about 1 cm and the QE is measured in the center of the MCP-PMTs, except for the XP85112/A1-HGL which was measured twice: Once at the exposed pixels (22, 23, 32 and 33) and once at the covered area (pixel 57). Further information of the QE setup can be found in [10].

On larger time scales in the order of a few weeks, the space-resolved QE was determined. A PiLas of 372 nm allowed spot diameters of about 0.5 mm . The surface of every sensor was scanned along both directions with a step size of 0.5 mm .

3. Results

3.1 Gain and dark count rate

As expected the dark count rate has decreased for all sensors during the illumination process (see Fig. 1). The Hamamatsu R10754X-01-M16 decreased by two orders of magnitude after

²Hamamatsu S6337-01

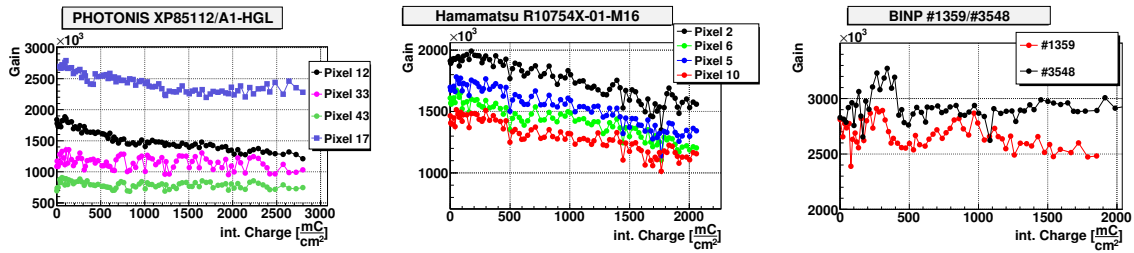


Figure 2: Gain as a function of the integrated anode charge. During the aging process pixel 17 of the XP85112/A1-HGL was covered

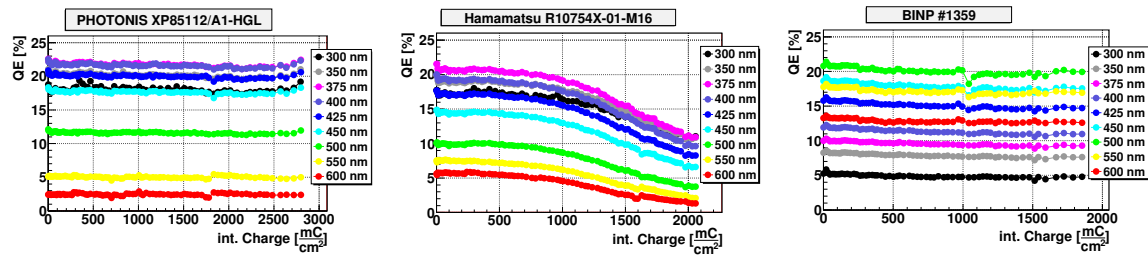


Figure 3: Quantum efficiency as a function of the integrated anode charge. The color code corresponds to the wavelength.

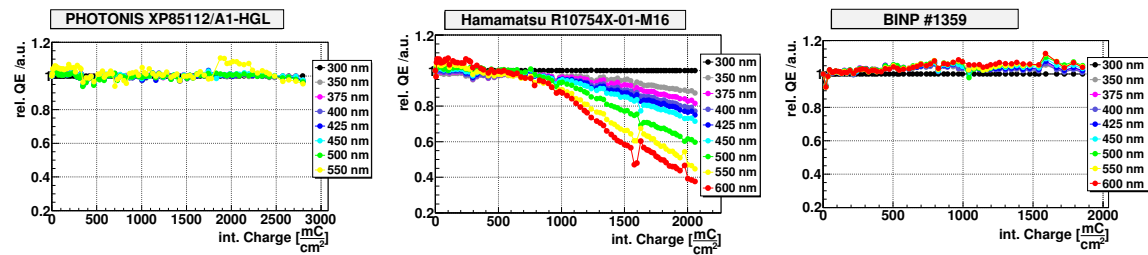


Figure 4: QE normalized to the degradation of the QE of 300 nm. The 'spikes' of R10754X-01-M16 at 1550 mC/cm^2 are artifacts after a Xe-lamp exchange.

2 C/cm^2 and has reached the detection threshold of about 1 cps. While the XP85112/A1-HGL dropped just at the beginning to a level of about 30% for the exposed pixels, the covered one (57) did not show any deviation at all. All exposed pixels stayed constant after the first drop up to the maximum charge of 2.8 C/cm^2 . A declining dark count rate could be observed for the Russian devices as well. The lower rate of the #3548 can be explained by the manufacturing process, which was longer baked in Cs/Sb vapor.

The gain (see Fig. 2) dropped by about 10-20% for the XP85112/A1-HGL (both exposed and unexposed pixels) and about 25% for the R10754X-01-M16, respectively. Both Russian devices on the other hand did not show any change. Previous measurements [7] [9] indicated a rather fast drop of about 50% at the beginning - this difference is not yet understood.

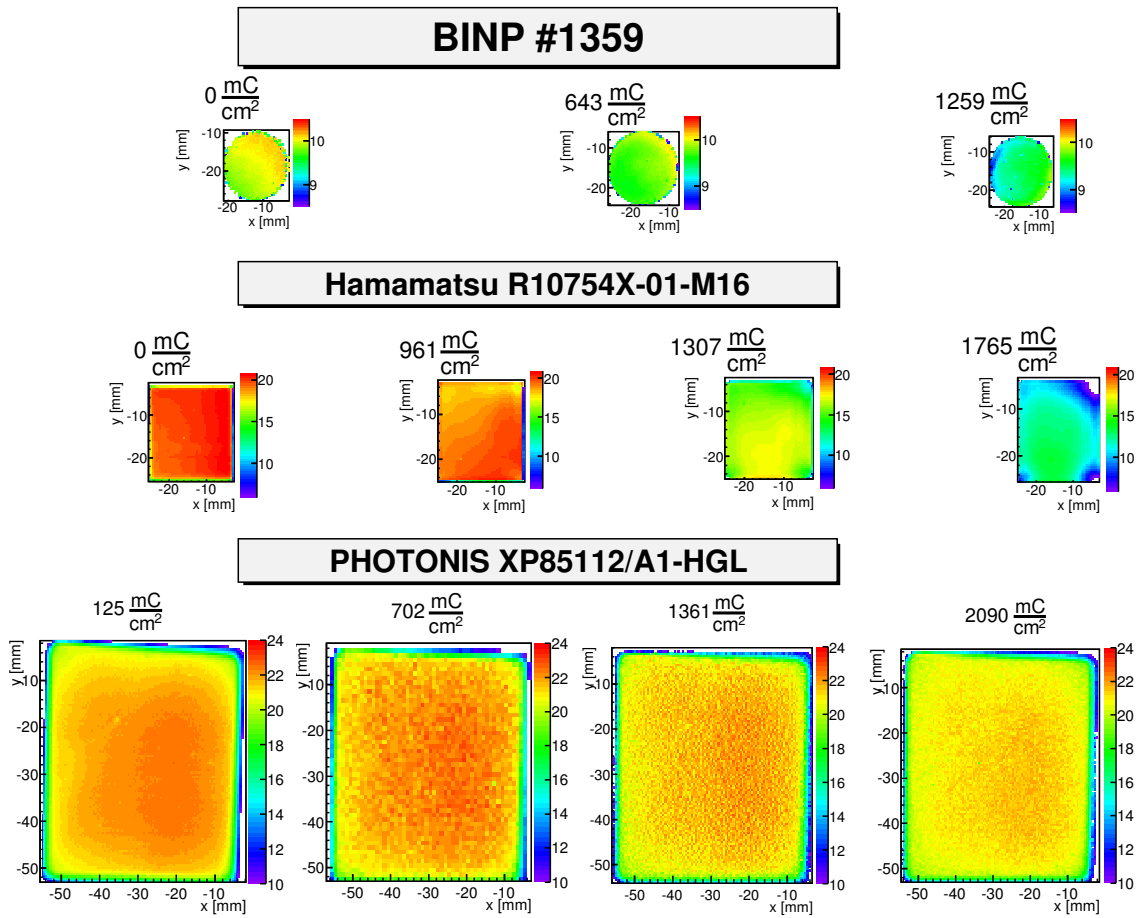


Figure 5: QE surface scan at 372 nm at a step size is 0.5 mm. All dimensions are scaled to the size of the XP85112/A1-HGL

3.2 Spectral and spatial quantum efficiency

The most important aging parameter is the QE (see Fig. 3). For the XP85112/A1-HGL this was constant at all wavelengths up to the latest measurements at 2.8 C/cm^2 - e.g., the QE of 400 nm remained at 21.5%. The different photo cathode ($\text{Na}_2\text{KSb}(\text{CS}) + \text{Cs}_3\text{Sb}$, which is most sensitive at about 500 nm) of the Russian MCPs started at a lower value and dropped slowly and constantly from 12.2% to 11% for the #1359 after 1.85 C/cm^2 (resp. 12.2% to 10.8% after 2.06 C/cm^2 for the #3548). Unlike the others the QE of the R10754X-01-M16 was constant up to $\sim 0.8 \text{ C/cm}^2$ and decreased afterwards. The latest results at 400 nm show a QE decline from (absolute) 20% to 9.6%, which corresponds to a relative drop by 52%.

The standard multi- and bi-alkali cathodes showed a faster drop for higher wavelengths in previous lifetime measurements [7] [9]. This behavior was revealed by normalizing all QEs of a sensor to a certain wavelength. As a reference the QE drop at 300 nm was chosen. Fig. 4 shows the data of the latest-generation MCP-PMTs. Obviously the XP85112/A1-HGL does not show any decline for higher wavelengths, which can only be explained with no degradation so far. The R10754X-01-M16 on the other hand dropped faster for higher wavelengths: the relative QE at 600 nm just

remained 38% compared to 300 nm (77% for 400 nm). Another key factor is a better knowledge of the starting point of the degradation, which can again be determined to $\sim 0.8 C/cm^2$. This is in good agreement to lifetime measurements of other groups [11]. Yet the BINP #1359 (and #3548, but not shown) behaved differently: although a measurable degradation is visible in Fig. 3, the QE drop is the same for all wavelengths, which is indicated in the flat lines of Fig. 4.

Last but not least the space-resolved QE at 372 nm can be seen in Fig. 5. All devices are plotted in their relative sizes of the photo cathode area. The BINP #1359 dropped from 10.2% to 9.2% and no signs of different aging areas were measured (#3548 behaves similar - not shown). The XP85112/A1-HGL remained constant across the whole surface at about 22% during the illumination. In contrast the aging of the R10754X-01-M16 started from the corners, especially the upper right, which can probably be explained by an imperfect ceramic insulation of the MCP for bypassing ions. Ref. [11] described this problem in more detail.

4. Summary and conclusion

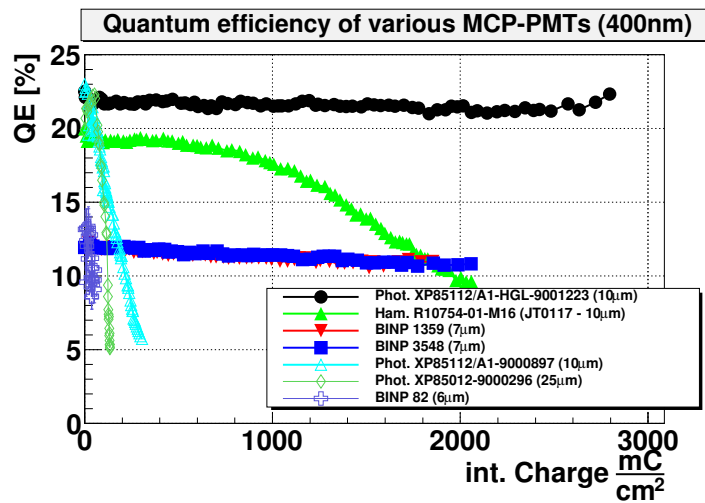


Figure 6: Quantum efficiency of all measured MCP-PMTs as a function of the integrated anode charge, plotted for old (open dots) and new (solid dots) devices

#1359 and #3548 dropped relatively by about 10% (after $1.85 C/cm^2$ resp. $2.06 C/cm^2$), while the XP85112/A1-HGL did not show any degradation even after $2.8 C/cm^2$. Only the R10754X-01-M16 was not able to survive that long, resulting in a relative drop of 50% after $2.0 C/cm^2$.

Our measurements clearly show the best lifetime performance for the ALD-coated MCP-PMT, resulting in a huge benefit when comparing XP85112/A1-HGL to its direct predecessor XP85112/A1 produced without ALD coating. Taking into account the expected integrated anode charge of $5 C/cm^2$ at the $\bar{P}ANDA$ barrel DIRC, using MCP-PMTs as photo sensors are rather within reach.

All of the latest improvements in the manufacturing process of MCP-PMTs increased their lifetime compared to devices available some years ago. In Fig. 6 the QEs of all measured devices are shown. The first measured BINP #82 had an aluminum oxide layer at the first MCP layer, reducing the collection efficiency. All predecessor MCP-PMTs were not able to stand integrated anode charges of more than $200 mC/cm^2$. However, concerning the latest-generation MCP-PMT devices the BINP

5. Acknowledgements

We want to thank our colleagues of ECAP³ - O. Kalekin and B. Herold - for their help and use of the QE setup. Many thanks for M. Barnyakov for lending both BINP tubes and PHOTONIS, especially E. Schyns and J. DeFazio, for useful conversations. This work is supported by German BMBF and GSI.

References

- [1] Paola Gianotti, *The PANDA Experiment at FAIR*, Nucl. Phys. A **835** (2010) 96-101
- [2] D. Bettoni et al., PANDA Collaboration *Physics Performance Report for PANDA: Strong Interaction Studies with Antiprotons*, (2009) [hep-ex/0903.3905v1]
- [3] PANDA collaboration, *Technical progress report for PANDA. Strong interaction studies with anti-protons*, FAIR-ESAC/Pbar 2005
- [4] J. Schwiening et al., *The barrel DIRC detector for the \bar{P} ANDA experiment at FAIR* Nucl. Instrum. Meth. A **639** (2011) 315-318 <http://dx.doi.org/10.1016/j.nima.2010.10.061>
- [5] C. Schwarz et al., *The Barrel DIRC of PANDA*, in *Workshop on fast Cerenkov detectors - Photon detection, DIRC design and DAQ (DIRC2011)*, April 4-6, Giessen, Germany, *JINST* **7** C02008 (2012) <http://dx.doi.org/10.1088/1748-0221/7/02/C02008>
- [6] M. Düren et al., *The PANDA 3D Disc DIRC*, in *Workshop on fast Cerenkov detectors - Photon detection, DIRC design and DAQ (DIRC2011)*, April 4-6, Giessen, Germany, *JINST* **7** C01068 (2012) <http://dx.doi.org/10.1088/1748-0221/7/01/C01059>
- [7] A. Lehmann et al., *Systematic studies of micro-channel plate PMTs* Nucl. Instrum. Meth. A **639** (2011) 144-147 <http://dx.doi.org/10.1016/j.nima.2010.09.071>
- [8] A. Lehmann et al., *Performance studies of microchannel plate PMTs in high magnetic fields* Nucl. Instrum. Meth. A **595** (2007) 173-176 <http://dx.doi.org/10.1016/j.nima.2008.07.083>
- [9] A. Britting et al., *Lifetime-issues of MCP-PMTs*, in *Workshop on fast Cerenkov detectors - Photon detection, DIRC design and DAQ (DIRC2011)*, April 4-6, Giessen, Germany, *JINST* **6** C10001 (2011) <http://dx.doi.org/10.1088/1748-0221/6/10/C10001>
- [10] O. Kalekin et al., *PMT characterization for the KM3NET project* Nucl. Instrum. Meth. A **626-627** (2011) 151-153 <http://dx.doi.org/10.1016/j.nima.2010.04.129>
- [11] T. Mori et al., *Lifetime-extended MCP-PMT* Nucl. Instrum. Meth. A **629** (2011) 111-117 <http://dx.doi.org/10.1016/j.nima.2010.10.145>

³Erlangen Center of Astroparticle Physics